

Pyrolysis of Polycyclic α,ω -Diarylpropanes Pathways, Kinetics, and Mechanisms

C. Michael Smith and Phillip E. Savage
Department of Chemical Engineering
The University of Michigan
Ann Arbor, MI 48109-2136

Division of Fuel Chemistry
Symposium on Model Compounds in Coal Liquefaction
American Chemical Society
Boston, MA Meeting
April 1990

INTRODUCTION

α,ω -Diphenylalkanes have been commonly used as chemical models of the scissile aliphatic linkages between aromatic moieties in coal (e.g., Vernon, 1980; Poutsma and Dyer, 1982; Gilbert and Gajewski, 1982; Sweeting and Wilshire, 1962; Miller and Stein, 1981). In coal, of course, the terminal aromatic moieties are generally neither single ringed nor identical, thus unsymmetrical polycyclic α,ω -diarylalkanes might better mimic these moieties. Studies of these apparently relevant model compounds are few, however. The most probable reason for this gap in the literature stems from the reasoning that the reaction pathways, kinetics, and mechanisms of polycyclic α,ω -diarylalkanes can be extrapolated from those of single ring α,ω -diphenylalkanes. Indeed, the limited previous studies (e.g., Vernon, 1980; Sato, 1979; Javanmardian et al., 1988; Depp et al., 1956) with polycyclic α,ω -diarylalkanes suggest that this premise is reasonable. For example, Javanmardian et al. (1988) reported that the pyrolysis pathway for 2-(3-phenylpropyl)-naphthalene (PPN) led to toluene plus 2-vinylnaphthalene and 2-methylnaphthalene plus styrene; products analogous to those formed during 1,3-diphenylpropane pyrolysis. They further observed approximately equal molar yields of 1-methylnaphthalene and toluene from PPN pyrolysis suggesting that the presence of the naphthyl moiety in a 1,3-diarylalkane had little effect on the selectivity. It did, however, increase the rate of pyrolysis in comparison to that observed for 1,3-diphenylpropane.

In the present work, we further probe the pyrolysis pathways and kinetics of polycyclic α,ω -diarylalkanes. In particular, we present results of pyrolysis studies of two α,ω -diarylpropanes: 2-(3-phenylpropyl)-naphthalene (PPN) and 1,3-bis-(1-pyrene)propane (BPP). This work was motivated by our recent findings that the pyrolysis pathways for *n*-alkyl-substituted pyrenes are markedly different than the pathways for *n*-alkyl-substituted benzenes (Savage et al., 1989; Smith and Savage, 1989). The key differences were the presence of apparent autocatalytic kinetics and the cleavage of the strong aryl-alkyl C-C bond as the pathway to the major products.

EXPERIMENTAL

The pyrolysis of PPN (API Standard Reference Materials) and BPP (Molecular Probes) both neat and in benzene were conducted in constant-volume, 316 stainless steel batch reactors. These reactors were made from one 1/4 in. Swagelok port connector and two 1/4 in. Swagelok end caps and had a volume of $0.59 \pm .05$ ml. For the PPN neat pyrolyses, the batch reactors were loaded with approximately 40 mg of a previously prepared stock solution of PPN and biphenyl (an internal standard), and for BPP neat pyrolyses the batch reactors were loaded with an average of 2.3 mg of BPP and 9.3 mg of biphenyl. For the pyrolyses in benzene, the batch reactors were loaded with approximately 350 mg of a previously prepared stock solution comprising the model compound, biphenyl, and benzene as the inert diluent. All quantities were carefully weighed with an analytical balance. For the pyrolyses in benzene, the reactant concentration was calculated as the number of moles of reactant added to the reactor divided by the reactor volume. After being purged with argon, the reactors were placed in an isothermal fluidized sand bath at the desired temperature (e.g., 400°C). Upon reaching the desired holding time, the reactors were removed from the sand bath and rapidly cooled in an ambient temperature water bath. The reactors were opened, and products were recovered by benzene extraction for BPP and acetone extraction for PPN. Products were identified using GC (HP 5890) and GC-MS (HP 5890 Series 11 - HP 5970 MSD) and quantified by GC using biphenyl as an internal standard. GC response factors for the reaction products were experimentally determined from standard solutions that contained the reaction products and biphenyl in varying amounts. Plotting the ratio of the mass of a particular compound to the mass of biphenyl in the solution as a function of the ratio of

their integrated GC areas resulted in a straight line and gave the response factor as the slope. The average error for these response factors was 3% (Noggle, 1985).

PPN PYROLYSIS

Experimental Results

Table 1 displays the molar yields of the major products from the neat pyrolysis of PPN at 365 and 400°C and the pyrolysis of PPN in benzene at 375, 400, and 450 °C. The principal products at low PPN conversions were toluene, 2-vinylnaphthalene, 2-methylnaphthalene and styrene, but at high PPN conversions, 2-ethylnaphthalene and ethylbenzene were also present in high yields. The presence of these products and their temporal variations are consistent with the reaction pathway previously determined by Javanmardian et al. (1988). There is, however, a discrepancy with the previous work. Our present work showed that the yields of toluene were higher than the yields of 2-methylnaphthalene, whereas, in the earlier work the yields of toluene and 2-methylnaphthalene were essentially equal. We suspect that the reason for this discrepancy stems from our taking a more careful approach in determining GC response factors for the observed reaction products. Javanmardian et al. (1988) used a single point calibration for the response factors whereas the present analysis used linear regression of at least five points.

The minor products from PPN pyrolysis included 1,3-diphenylpropane and 2-*iso*-propylnaphthalene, which were previously observed by Javanmardian et al. (1988), and naphthalene. The neat pyrolysis also led to the production of acetone-insoluble char. The amounts of this dark solid material increased with temperature and batch holding time. We expect that the formation of this char satisfies the global material balance.

Javanmardian et al. (1988) found that the neat pyrolysis of PPN correlated well with pseudo-first order kinetics. Thus, we calculated pseudo-first-order rate constants from our data and plotted them along with those of Javanmardian et al. (1988) on the Arrhenius plot given as Figure 1. Clearly, the present kinetics results for PPN neat pyrolysis are consistent with the previous work. The Arrhenius parameters determined by Figure 1 are $\log_{10} A = 9.6 \text{ sec}^{-1}$ and $E^* = 38.5 \text{ kcal mol}^{-1}$ for the neat pyrolysis and $\log_{10} A = 7.7 \text{ sec}^{-1}$ and $E^* = 35.2 \text{ kcal mol}^{-1}$ for the pyrolyses in benzene.

Reaction Mechanism

Our results from PPN pyrolysis and previous pyrolyses of its single ring analogue (Poutsma and Dyer, 1982; Gilbert and Gajewski, 1982) led us to propose the free-radical reaction mechanism in Figure 2 to describe PPN pyrolysis. The 18 step mechanism comprises initiation, propagation, and termination steps. Initiation entails the unimolecular dissociation of the weak C-C bonds in the reactant, and we included two possible initiation steps for PPN. The first route corresponds to the formation of benzyl and 2-ethylnaphthyl radicals (denoted β_1 and β_1' in Figure 2), and the second route leads to ethylbenzyl and 2-methylnaphthyl radicals (denoted β_2 and β_2' in Figure 2). Propagation occurs through abstraction of α hydrogens in PPN by β radicals and subsequent β -scission of the resulting radical, μ , to form a stable product Q and regenerate a β radical. Termination of the chain reaction can occur through all possible radical recombination steps.

Kinetics Development

The steady state and long chain approximations can be used to derive an analytical rate expression for the mechanism of Figure 2. The rate of reaction for PPN (denoted as R in Figure 2) is given by Equation 1.

$$-r_R = (k_{11} + k_{12})\beta_1 R + (k_{21} + k_{22})\beta_2 R \quad (1)$$

Expressions for β_1 and β_2 as functions of the rate constants and the reactant concentration can be obtained by writing the long chain rate expressions for β_1 , β_2 , μ_1 , and the total radical population ($R\cdot$). Equations 2-5 display these expressions.

$$r_{\beta_1} = k_{\mu_1} \mu_1 \cdot (k_{11} + k_{12})\beta_1 R = 0 \quad (2)$$

$$r_{\beta_2} = k_{\mu_2} \mu_2 \cdot (k_{21} + k_{22}) \beta_2 R = 0 \quad (3)$$

$$r_{\mu_1} = k_{11} \beta_1 R + k_{21} \beta_2 R - k_{\mu_1} \mu_1 = 0 \quad (4)$$

$$r_{R_0} = 2(\alpha_1 + \alpha_2) R \cdot 2\omega_T (\mu_1 + \mu_2 + \beta_1 + \beta_2)^2 = 0 \quad (5)$$

Simultaneous solution of Equations 2-5 provides the required expressions for β_1 and β_2 . These can then be substituted into Equation 1 to derive Equation 6 as the rate law for PPN disappearance.

$$-r_R = \frac{\sqrt{\frac{\alpha_1 + \alpha_2}{\omega_i}} \left[\left(\frac{k_{12}}{k_{21}} \right) (k_{21} + k_{22}) + (k_{11} + k_{12}) \right] R^{3/2}}{\left[\frac{(k_{11} + k_{12})}{k_{\mu_1}} + \left(\frac{k_{12}}{k_{21}} \right) \frac{(k_{21} + k_{22})}{k_{\mu_2}} \right] R + \left[1 + \left(\frac{k_{12}}{k_{21}} \right) \right]} \quad (6)$$

Defining the parameters ζ and ξ as

$$\zeta = \frac{\left[\frac{(k_{11} + k_{12})}{k_{\mu_1}} + \left(\frac{k_{12}}{k_{21}} \right) \frac{(k_{21} + k_{22})}{k_{\mu_2}} \right]}{\sqrt{\frac{\alpha_1 + \alpha_2}{\omega_i}} \left[\left(\frac{k_{12}}{k_{21}} \right) (k_{21} + k_{22}) + (k_{11} + k_{12}) \right]} \quad (7)$$

$$\xi = \frac{\left[1 + \left(\frac{k_{12}}{k_{21}} \right) \right]}{\sqrt{\frac{\alpha_1 + \alpha_2}{\omega_i}} \left[\left(\frac{k_{12}}{k_{21}} \right) (k_{21} + k_{22}) + (k_{11} + k_{12}) \right]} \quad (8)$$

permits the rate law (Equation 6) to be written in more compact form.

$$-r_R = \frac{R^{3/2}}{\zeta R + \xi} \quad (9)$$

Substituting this rate law into the constant volume batch reactor design equation, writing the reactant concentration as a function of conversion (i.e., $R = R_0(1-X)$), integrating, and rearranging, results in a simple expression for the batch holding time (t) as a function of conversion (X) and the initial PPN concentration (R_0).

$$t = \frac{2\xi}{\sqrt{R_0}} \left[\frac{1}{\sqrt{1-X}} - 1 \right] - 2\zeta \sqrt{R_0} \left[\sqrt{1-X} - 1 \right] \quad (10)$$

The mechanism of Figure 2 also permits derivation of an analytical expression for the product selectivity. The instantaneous selectivity (S) of PPN to toluene relative to 2-methynaphthalene is given as the ratio of the reaction rates.

$$S = \frac{r_{\text{TOL}}}{r_{2\text{-MN}}} = \frac{(k_{11} + k_{12}) \beta_1}{(k_{21} + k_{22}) \beta_2} \quad (11)$$

Substituting the relationship between β_1 and β_2 that results from the solution of Equations 2-5 into Equation 11 leads to Equation 12 for the instantaneous selectivity.

$$S = \frac{r_{\text{TOL}}}{r_{2\text{-MN}}} = \frac{\left(1 + \left(\frac{k_{11}}{k_{12}}\right)\right)}{\left(1 + \left(\frac{k_{22}}{k_{21}}\right)\right)} \quad (12)$$

Rate Constant Estimation

Employing Equations 10 and 12 to model the kinetics and selectivity of PPN pyrolysis requires values for each of the rate constants in the reaction mechanism shown in Figure 2. In the following paragraphs we describe our rate constant estimation procedures. Note that the values we used for the rate constants were semi-quantitative. More accurate estimates could be made using thermochemical kinetics.

Rate constants for initiation via homolytic dissociation of C-C bonds typically have pre-exponential factors in the range of $10^{16 \pm 1} \text{ s}^{-1}$ (Benson, 1976). Thus, we selected a value of $A = 10^{16} \text{ s}^{-1}$ for both of the initiation rate constants α_1 and α_2 . We used 69 kcal mol^{-1} as the activation energy for α_1 (which produces a benzyl and 2-ethylnaphthyl radical). This value is in good accord with the calculated bond dissociation energy (BDE) of $68.81 \text{ kcal mol}^{-1}$ for the identical bond in 1,3-diphenylpropane (King and Stock, 1984). The rate of initiation via step α_2 will be faster than via step α_1 because the additional resonance stabilization energy associated with the naphthyl moiety reduces the BDE of the benzylic C-C bond. Thus, the activation energy for this step was taken to be $E^* = 69 - \Delta\text{RSE}$, where ΔRSE is the difference in the resonance stabilization energies between a 2-methylnaphthyl radical and a benzyl radical. We used Sato's calculated value of $0.41 \text{ kcal mol}^{-1}$ for the ΔRSE .

Hydrogen abstraction rate constants were estimated by first assuming that the pre-exponential factors for k_{11} , k_{12} , k_{21} , and k_{22} were all equal to $A = 10^8 \text{ l mol}^{-1} \text{ s}^{-1}$ and that the activation energy for k_{12} was $14.2 \text{ kcal mol}^{-1}$. These Arrhenius parameters for k_{12} are identical to those estimated by Poutsma and Dyer (1982) for abstraction of a secondary benzylic hydrogen by a primary benzyl radical. The activation energy for k_{21} was also taken as $14.2 \text{ kcal mol}^{-1}$ because the reduction in rate for this step relative to k_{12} due to the increased stability of the abstracting radical (i.e., 2-methylnaphthyl vs. benzyl) should be roughly offset by the increase in rate due to the lower C-H bond strength of the β -position being attacked. Finally the activation energies for k_{11} and k_{22} were estimated from the activation energies for k_{21} and k_{12} by assuming that half of the ΔRSE associated with the two different hydrogens being abstracted radicals would appear as the activation energy difference. This is essentially the same as employing the Evans-Polanyi relation with $\alpha=0.5$, a value commonly used (Stein, 1985; Poutsma and Dyer, 1982) for hydrogen abstraction reactions.

Poutsma and Dyer (1982) estimated the Arrhenius parameters for β -scission of an α -radical in 1,3-diphenylpropane to be $A = 10^{14.8} \text{ s}^{-1}$ and $E^* = 28.3 \text{ kcal mol}^{-1}$. For PPN pyrolysis, we expect $k_{\mu 1}$ to be lower than the β -scission rate constant for 1,3-diphenylpropane pyrolysis because the μ_1 radical should be more stable than the corresponding 1,3-diphenylpropane-derived radical. On the other hand, we expect $k_{\mu 2}$ to be higher because the additional RSE due to the presence of the naphthyl moiety in PPN results in the β -scission of a weaker C-C bond. We quantified the foregoing qualitative arguments by taking $10^{14.8} \text{ s}^{-1}$ as the pre-exponential factor for the β -scission steps and using $28.2 \text{ kcal mol}^{-1}$ as the activation energy for $k_{\mu 1}$ and $28.4 \text{ kcal mol}^{-1}$ as E^* for $k_{\mu 2}$.

Termination rate constants for radical recombination generally have zero activation energy and pre-exponential factors of $A = 10^{9.0 \pm 1} \text{ l mol}^{-1} \text{ s}^{-1}$ (Benson, 1976). For our termination rate constant, ω_T , we used $A = 10^{8.5}$ and $E^* = 0.0 \text{ kcal mol}^{-1}$.

Modeling Results

We used the semi-quantitative rate constant estimates described above as parameters in Equations 10 and 12 to calculate the kinetics and selectivity for PPN pyrolysis under the conditions at which we had performed experiments. Figure 3 compares the calculated and experimentally determined temporal variation of the PPN molar yield for the pyrolyses in benzene. Clearly, the kinetics predicted from the reaction model are in good agreement with the experimental data. Figure 4 provides the calculated and experimentally determined instantaneous selectivity of PPN to toluene relative to 2-methylnaphthalene. The data points were calculated as the mean values for all batch holding times at a given temperature. Once again, we find satisfactory agreement between the results of the reaction model and the experiments.

BPP PYROLYSIS

Experimental Results

Table 2 provides the molar yields of the major products from the pyrolysis of BPP neat at 365°C and in benzene at 400°C. The major products from pyrolysis in benzene at short batch holding times (e.g., 10 min), were 1-methylpyrene and 1-vinylpyrene. At long times, however, the yield of 1-vinylpyrene decreased while the yield of 1-ethylpyrene increased. Additionally, pyrene became a major product at the longer holding times. Figure 5, which presents the temporal variations of the product yields for BPP pyrolyses in benzene, displays these trends more clearly.

The neat pyrolysis of BPP led to 1-methylpyrene, 1-ethylpyrene, and pyrene as principal products. No vinylpyrene was detected, but trace amounts of 1-propylpyrene and 1-allylpyrene were observed along with visible amounts of benzene-insoluble char. At a batch holding time of 90 minutes the respective molar yields for 1-methylpyrene, 1-ethylpyrene, and pyrene were 62%, 40% and 23% respectively.

Reaction Pathway

The initial products formed from BPP pyrolysis were 1-methylpyrene and 1-vinylpyrene. These are analogous to toluene and styrene, the primary products of 1,3-diphenylpropane pyrolysis. The coincidence of initial products indicates that the pathway for BPP pyrolysis at short times is identical to the pyrolysis pathway for its single ring analogue, 1,3-diphenylpropane. At longer times and higher concentrations, however, the pyrolysis of BPP led to the formation of appreciable yields ($\geq 30\%$) of pyrene. Similarly high yields of benzene have never been observed from 1,3-diphenylpropane pyrolysis. The pathways responsible for pyrene formation can be inferred from the temporal variations of the product yields illustrated in Figure 5. The molar yields of methylpyrene and ethylpyrene both decreased at the longer holding times where the molar yield of pyrene increased. Thus, it appears that ethylpyrene and methylpyrene underwent secondary reactions that resulted in the loss of their alkyl substituents at the aromatic ring. Such a pathway is entirely consistent with our recent studies of 1-dodecylpyrene pyrolysis (Savage et al., 1989; Smith and Savage 1989) where aryl-alkyl C-C bond cleavage was an important reaction pathway. The amount of pyrene formed, however, may be too high to be the sole result of secondary decomposition reactions of methyl- and ethylpyrene. This suggests that BPP itself may have undergone primary reaction to form pyrene. The precise mechanism for these pathways involving cleavage of strong aryl-alkyl C-C bonds is currently unknown, although the literature does provide some possibilities (e.g., Vernon, 1980; McMillen et al., 1987). Indeed, our earlier work with 1-dodecylpyrene pyrolysis (Smith and Savage, 1989) suggests that radical hydrogen transfer may be responsible for the cleavage of the strong aryl-alkyl C-C bonds during alkyl-pyrene pyrolysis. Figure 6 summarizes the foregoing discussion by displaying the postulated pyrolysis pathways for BPP. Note that the presence of pathways involving aryl-alkyl bond cleavage is a completely new feature of α,ω -diarylpropane pyrolysis.

CONCLUSIONS

1. The pyrolysis pathways for α,ω -diarylalkanes and hence the corresponding moieties in coal have not been completely elucidated. BPP, a polycyclic diarylalkanes, followed a pyrolysis pathway where strong aryl-alkyl C-C bonds were cleaved. This appearance of this new pathway clearly

indicates that the complete pyrolytic behavior of α,ω -diarylpropanes can not always be inferred from 1,3-diphenylpropane.

- For the pyrolysis of PPN, aryl-alkyl cleavage was not a major pathway. The pathways and mechanisms for PPN pyrolysis can be inferred from knowledge of 1,3 diphenylpropane pyrolysis. Furthermore, the reaction kinetics and product selectivities can be accurately calculated for by the accounting for the relevant resonance stabilization energy differences.

NOTATION

A	pre-exponential factor, (l/s, l/mol-s)
E [‡]	activation energy, (kcal/mol)
k _{μi}	β -scission rate constant, (l/s)
k _{ij}	hydrogen abstraction rate constant, (l/mol-s)
Q	reaction product in Figure 2
r	reaction rate, (mol/l-s)
R	reactant in Figure 2 or reactant concentration, (mol/l)
R ₀	initial reactant concentration, (mol/l)
t	batch holding time, (s)
X	reactant conversion
α_i	initiation rate constant, (l/s)
β_i	radical reacting in bimolecular propagation step
β_iH	stable product in Figure 2, (mol/l)
μ_i	radical reacting in unimolecular propagation step
C_i^*	parameters in equation 10
ω_T	termination rate constant, (l/mol-s)

LITERATURE CITED

- Benson, S. W. *Thermochemical Kinetics* John Wiley and Sons, New York, 1976.
- Depp, E. A., Stevens, C. M., Neuworth, M. B. Pyrolysis of Bituminous Coal Models *Fuel*, 1956, 35, 437.
- Gilbert, K.E., Gajewski, J. J. Coal Liquefaction Model Studies: Free Radical Chain Decomposition of Diphenylpropane, Dibenzyl Ether, and Phenyl Ether via β -Scission Reactions. *J. Org. Chem.*, 1982, 47, 4899.
- Javanmardian, M., Smith, P.J., Savage, P. E. Pyrolysis of Compounds Containing Polycyclic Aromatic Moieties. *Prepr.-Am. Chem. Soc., Div. Fuel. Chem.* 1988,33,242.
- King, H., Stock, L.M. Aspects of the Chemistry of Donor Solvent Coal Dissolution *Fuel*, 1984, 63, 810.
- McMillen, D. F., Malhorta, R., Chang, S.J., Olgier, W.C., Nigenda, E, Fleming, R. H. Mechanisms of Hydrogen Transfer and Bond Scission of Strongly Bonded Coal Structures in Donor-Solvent Systems. *Fuel*, 1987, 66, 1611.
- Miller, R. E., Stein, S. E. Liquid-Phase Pyrolysis of 1,2 Diphenylethane, *J. Phys. Chem.*, 1982, 580.
- Noggle, J. H. *Physical Chemistry* Little, Brown, and Company, Boston 1985.

- Poutsma, M. L., Dyer, C. W. Thermolysis of Model Compounds for Coal. 3. Radical Chain Decomposition of 1,3-Diphenylpropane and 1,4-Diphenylbutane, *J. Org. Chem.*, 1982, 47, 4903.
- Sato, Y. Dissociation Energies of C-C Bonds in Bibenzyl and 1,2-di-1-Naphthylethane *Fuel*, 1979, 58, 318
- Savage, P.E., Jacobs, G.E., Javanmardian, M. Autocatalysis and Aryl-Alkyl Bond Cleavage in 1-Dodecylpyrene Pyrolysis *Ind. Eng. Chem. Res.*, 1989, 28, 645.
- Smith, C. M., Savage, P. E. Pyrolysis of Alkyl-Substituted Polycyclic Aromatic Compounds Paper 93d Presented at AIChE Annual Meeting, San Francisco, CA November, 1989.
- Stein, S. E. Free Radicals in Coal Conversion in Chemistry of Coal Conversion, Edited by Richard Scholsberg, 1985, 13.
- Sweeting, J. W., Wilshire, J. F. K. The pyrolysis of $\omega\omega'$ -Diphenylalkanes *Aust. J. Chem.*, 1962, 15, 89.
- Vernon, L. W. Free Radical Chemistry of Coal Liquefaction: Role of Molecular Hydrogen *Fuel*, 1980, 59, 102.

ACKNOWLEDGEMENTS

This work was supported, in part, by the Shell Faculty Career Initiation Fund, an Energy Research Grant from the University of Michigan Office of the Vice President for Research, and the National Science Foundation (Grant No. CTS-8906859)

Table 1: Summary of PPN Pyrolysis Data
Molar Yields (%) of Products at Different Reaction Conditions

Time	Temp. °C	Conditions	TOL	STY	EB	MN	EN	VN	PPN
40	365	Neat	17.4	4.9	1.5	14.4	2.3	2.2	53.2
40	365	Neat	18.0	4.6	1.6	15.0	2.5	2.2	52.8
46	365	Neat	19.0	4.4	2.1	16.9	3.3	2.0	46.4
76	365	Neat	30.1	3.2	4.9	24.9	6.8	1.5	26.7
99	365	Neat	39.0	0.8	3.1	29.8	10.1	1.1	19.2
158	365	Neat	49.0	1.0	16.3	35.9	17.5	0.5	8.0
11	400	Neat	17.1	8.9	1.4	16.5	2.7	4.5	49.9
17	400	Neat	29.3	9.4	4.7	28.0	7.7	3.3	22.9
31	400	Neat	49.1	3.2	13.2	37.3	15.2	1.2	6.6
47	400	Neat	52.5	1.3	18.1	40.3	18.7	0.0	5.9
105	400	Neat	61.0	0.0	23.3	41.9	19.7	0.0	0.0
151	400	Neat	61.5	0.0	24.3	41.9	19.7	0.0	0.0
10	375	0.12 M Benzene	0.7	0.7	0.0	0.6	0.0	1.0	98.7
30	375	0.12 M Benzene	1.8	1.5	0.0	1.5	0.0	2.2	97.5
60	375	0.12 M Benzene	3.4	2.6	0.0	2.9	0.3	3.8	93.9
95	375	0.12 M Benzene	6.5	4.9	0.4	5.6	1.1	6.8	84.5
150	375	0.12 M Benzene	10.0	7.3	0.7	9.2	1.7	9.4	76.1
240	375	0.12 M Benzene	24.5	11.9	3.6	23.3	7.1	11.7	42.3
20	400	0.12 M Benzene	4.4	3.4	0.0	3.6	0.4	4.8	88.3
30	400	0.12 M Benzene	11.9	8.1	1.3	10.0	2.7	9.6	71.1
45	400	0.12 M Benzene	13.0	9.1	1.1	11.2	2.0	11.3	68.5
60	400	0.12 M Benzene	17.5	11.8	1.6	15.2	2.9	14.2	58.4
60	400	0.12 M Benzene	24.6	11.8	4.9	21.1	8.7	11.7	41.3
90	400	0.12 M Benzene	22.2	13.1	2.6	19.8	4.8	14.4	47.7
150	400	0.12 M Benzene	35.6	9.3	8.4	32.5	12.6	8.2	17.1
153	400	0.12 M Benzene	32.8	9.9	7.4	29.7	11.3	9.1	23.3
10	450	0.12 M Benzene	9.1	6.9	0.7	7.9	1.2	9.7	77.0
15	450	0.12 M Benzene	20.8	12.6	2.6	19.2	4.1	16.5	46.6
30	450	0.12 M Benzene	32.6	9.5	8.7	30.3	12.5	9.9	12.9
45	450	0.12 M Benzene	34.7	9.3	10.6	31.4	16.0	8.9	6.7
60	450	0.12 M Benzene	34.9	0.7	15.8	31.1	18.8	0.6	1.2
90	450	0.12 M Benzene	35.2	0.6	15.0	31.1	18.5	0.5	0.7

Table 2: Summary of BPP Pyrolysis Data
Molar Yields (%) of Products at Different Reaction Conditions

Time	Temp. °C	Conditions	Pyrene	Methylpyrene	Ethylpyrene	Vinylpyrene
10	365	Neat	5.5	34.1	23.9	
20	365	Neat	9.1	43.5	31.1	
40	365	Neat	16.7	58.1	40.9	
50	365	Neat	17.2	63.4	45.4	
90	365	Neat	23.0	61.7	39.6	
155	365	Neat	25.9	52.3	29.9	
10	400	0.005 in Benzene	0.8	3.7	2.3	5.9
20	400	0.005 in Benzene	1.4	10.4	8.2	7.0
30	400	0.005 in Benzene	2.0	15.7	12.0	7.1
45	400	0.005 in Benzene	1.6	15.9	11.4	7.1
60	400	0.005 in Benzene	4.0	35.5	31.0	7.6
120	400	0.005 in Benzene	7.7	51.2	48.5	3.5
180	400	0.005 in Benzene	11.6	56.2	54.3	1.2
240	400	0.005 in Benzene	16.0	62.9	58.3	0.0
411	400	0.005 in Benzene	23.9	60.8	53.4	0.0
816	400	0.005 in Benzene	36.0	42.1	34.2	0.0

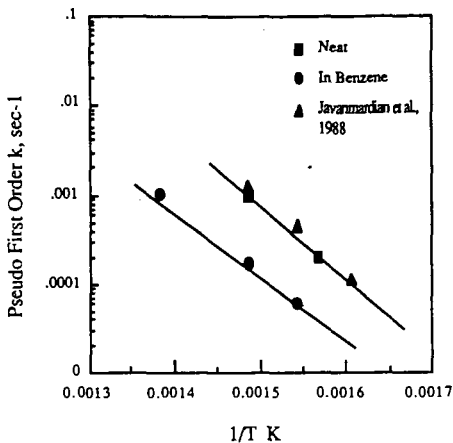


Figure 1: Arrhenius Plot for PPN Pyrolysis

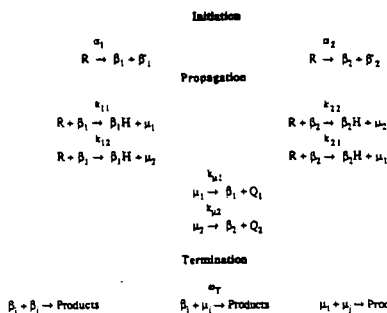


Figure 2: PPN Reaction Mechanism

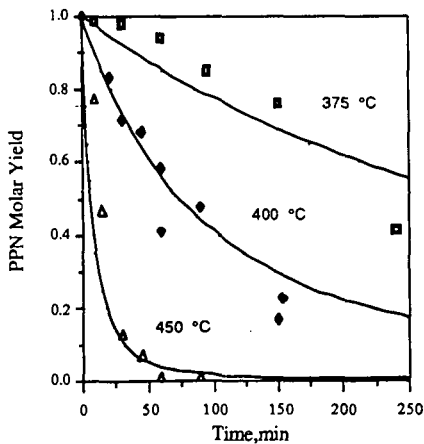


Figure 3: Modeling and Experimental Results for PPN Pyrolysis in Benzene 0.12M

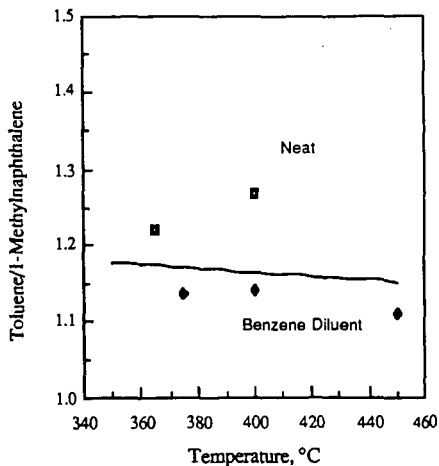


Figure 4: Model Predictions for PPN Pyrolysis Selectivity

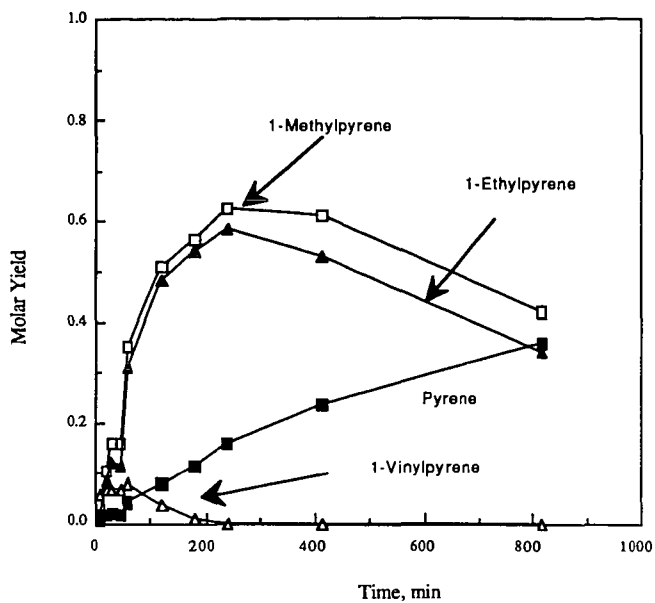


Figure 5: Molar Yields of Major Products for BPP Pyrolysis in Benzene (0.005 M, 400°C)

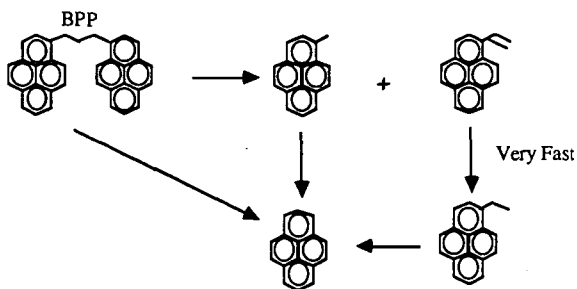


Figure 6: BPP Pyrolysis Pathway